

LASER APPLICATIONS AND OTHER TOPICS IN QUANTUM ELECTRONICS

PACS numbers: 85.60.Bt; 78.20.Jq
DOI: 10.1070/QE2014v044n04ABEH015317

Method for studying the phase function in tunable diffraction optical elements

V.D. Paranin, K.N. Tukmakov

Abstract. **A method for studying the phase function in tunable diffraction optical elements is proposed, based on measurement of the transmission of interelectrode gaps. The mathematical description of the method, which is approved experimentally, is developed. The instrumental error effects are analysed.**

Keywords: *tunable diffraction optical element, linear electrooptic effect, phase function, mathematical model.*

1. Introduction

Tunable diffraction optical elements (TDOEs) are constructed using electrooptic materials. The control of such elements consists in changing their directional pattern or spatiospectral function under the action of an electric field. To implement various directional patterns the electrodes are used, which are formed on the surface of an electrooptic material and have various topology and potential distributions. The TDOEs are largely employed in the design of electrooptic deflectors [1–3], modulators [4–6], controlled spectral filters [7, 8] and adaptive Fresnel lenses [9, 10]. Thus, TDOEs are used in information-controlling and measuring systems, as well as in locators and navigation complexes.

Further progress of TDOEs is restrained by a number of unsolved problems. The directional pattern of TDOEs is determined by the amplitude–phase transmission of the element. The amplitude transmission is measured using direct methods, while there are no methods for measuring the phase function in the interelectrode gaps of TDOEs. In the papers cited above the phase function was specified by using model electric field distributions in the electrooptic material. These models are based on the Laplace equation and do not account for possible repolarisation processes in the surface layer, as well as for dependence of the dielectric constant on the electric field strength and temperature.

The aim of this paper was to develop a method for studying experimentally the phase function and to approve it in the TDOE based on a lithium niobate electrooptic crystal.

2. Mathematical description of the method

The phase function was studied by measuring the TDOE interelectrode gap transmission. It is known that the application of control voltage affects the transmission by changing the polarisation state of the radiation, passing through the structure that consists of a polariser, a birefringent electrooptic crystal and an analyser. The process of phase function determination consists of two steps. First, the wave path length difference (WPLD) introduced by the electrooptic crystal is measured in the absence of electric voltage. Second, the transmission of the TDOE interelectrode gap is determined under the voltage applied. Since the WPLD determines the initial operating point of the voltage-transmission characteristic, it is possible to establish a unique relation between the interelectrode gap transmission and the desired phase function.

Note that both steps should be performed using the same radiation source, and the measurements should be carried out in the same local area of the crystal. Therefore, the known methods of the WPLD measurement [11, 12], which imply moving the crystal to a sample stage of an external measuring instrument, are not applicable.

The measurement is to be performed with the fixed polariser and crystal and the rotating analyser. The angle between the polariser axis and the crystal optical axis amounts to $\pi/4$. A schematic diagram of the WPLD measurement is presented in Fig. 1.

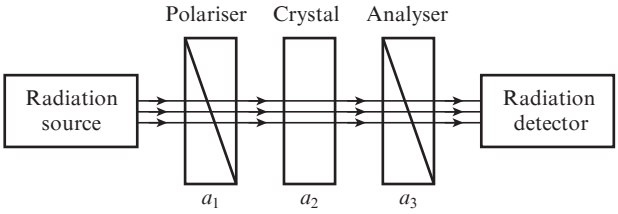

Figure 1. Schematic diagram for measuring the wave path length difference.

Radiation from a stabilised source enters the polariser–crystal–analyser system. Since the angles of rotation of the polariser a_1 and the crystal a_2 differ by $\pi/4$, the equal-intensity ordinary and extraordinary waves with the refractive indices n_o and n_e, respectively, are excited in the crystal. They determine the polarisation of radiation that leaves the crystal, depending on its thickness h. The output polarisation was controlled by rotating the analyser, and the optical radiation power was measured with a calibrated photodetector. To eliminate the influence of interference in the plane-parallel crystal plate, an incoherent radiation source should be used for the measurement.

Let us denote the rotation angles of the polariser, crystal, and analyser by a_1, a_2, and a_3, and their intensity transmission

V.D. Paranin, K.N. Tukmakov S.P. Korolev Samara State Aerospace University (National Research University), Moskovskoye sh. 34, 443086 Samara, Russia; e-mail: vparanin@mail.ru, Tukmakov.k@gmail.com

Received 22 September 2013; revision received 8 February 2014
Kvantovaya Elektronika **44** (4) 371–375 (2014)
Translated by V.L. Derbov

coefficients by t_1, t_2, and t_3. The amplitude and the power of the input radiation will be denoted by A_{in} and P_{in}, and the phases of the ordinary and the extraordinary wave will be denoted by φ_x and φ_z. Let us construct the Jones matrices for the optical elements, assuming that m_1, m_2, m_3 correspond to the analyser, m_4, m_5, m_6 correspond to the electrooptic crystal, and m_7, m_8, m_9 correspond to the polariser:

$$m_1 = \begin{pmatrix} \cos a_3 & -\sin a_3 \\ \sin a_3 & \cos a_3 \end{pmatrix}, m_2 = \begin{pmatrix} 1 & 0 \\ 0 & 0 \end{pmatrix}, m_3 = \begin{pmatrix} \cos a_3 & \sin a_3 \\ -\sin a_3 & \cos a_3 \end{pmatrix},$$
$$m_4 = \begin{pmatrix} \cos a_2 & -\sin a_2 \\ \sin a_2 & \cos a_2 \end{pmatrix}, \quad m_5 = \begin{pmatrix} \exp(j\varphi_x) & 0 \\ 0 & \exp(j\varphi_z) \end{pmatrix},$$
$$m_6 = \begin{pmatrix} \cos a_2 & \sin a_2 \\ -\sin a_2 & \cos a_2 \end{pmatrix}, \quad m_7 = \begin{pmatrix} \cos a_1 & -\sin a_1 \\ \sin a_1 & \cos a_1 \end{pmatrix}, \quad (1)$$
$$m_8 = \begin{pmatrix} 1 & 0 \\ 0 & 0 \end{pmatrix}, \quad m_9 = \begin{pmatrix} \cos a_1 & \sin a_1 \\ -\sin a_1 & \cos a_1 \end{pmatrix}.$$

According to the Jones matrix technique, the amplitudes of x- and z-polarised light waves A^x_{out}, A^z_{out} at the output of the polariser–crystal–analyser structure are related to the amplitudes of the source radiation polarised components A^x_{in}, A^z_{in} via the matrices (1):

$$\begin{pmatrix} A^x_{out} \\ A^z_{out} \end{pmatrix} = \prod_{i=1}^{9} m_i \begin{pmatrix} A^x_{in} \\ A^z_{in} \end{pmatrix}. \quad (2)$$

After multiplying the matrices m_i in Eqn (2) the output optical power takes the form

$$P_{out} = P^x_{out} + P^z_{out} = \frac{P_{in} t_1 t_2 t_3}{2}\left[1 + \cos(2a_3)\cos\left(\frac{2\pi}{\lambda} h\Delta n\right)\right], \quad (3)$$

where P_{in} is the power of the radiation source (mW).

The measurements of the output radiation power $P_{out}/P_{in}t_1t_2t_3$ versus the analyser rotation angle a_3 at different WPLD values in the crystal are illustrated in Fig. 2. The thickness h of the modelled crystals is expressed in the units of the characteristic thickness $\lambda/\Delta n$.

If the WPLD introduced by the crystal is a multiple of $\lambda/(4\Delta n)$ (a quarter-wave phase plate), then the polarisation state at the output is circular, and the components P^x_{out}, P^z_{out} are equal for all positions a_3 of the analyser. If the WPLD is a multiple of $\lambda/(2\Delta n)$ (a half-wave phase plate), then the output polarisation state is linear, and the variation of $P_{out}(a_3)$ versus a_3 is maximal. The change in the WPLD by $\lambda/(2\Delta n)$ leads to the shift of the characteristic by the angle $a_3 = \pi/2$.

Two methods for measuring the WPLD in the crystal follow from the dependences shown in Fig. 2. The first method is based on calculation of the slope of the characteristic curve $P_{out}(a_3)$ in the position $a_3 = \pi/4$, and the second one is based on determination of the ratio of the minimal and the maximal transmission at $a_3 = \pi/2$ and $a_3 = 0$. The advantage of both methods is the immobility of the radiation source and the crystal, which allows elimination of errors, related to nonuniformity of the radiation directional pattern and variations in the local properties of the electrooptic crystal.

Let us proceed to the mathematical description of the minimum–maximum method, since it is more stable with respect to angle adjustment errors of the measuring scheme elements. According to Eqn (3), the extrema of the output power $P_{out}(a_3)$ are expressed as follows:

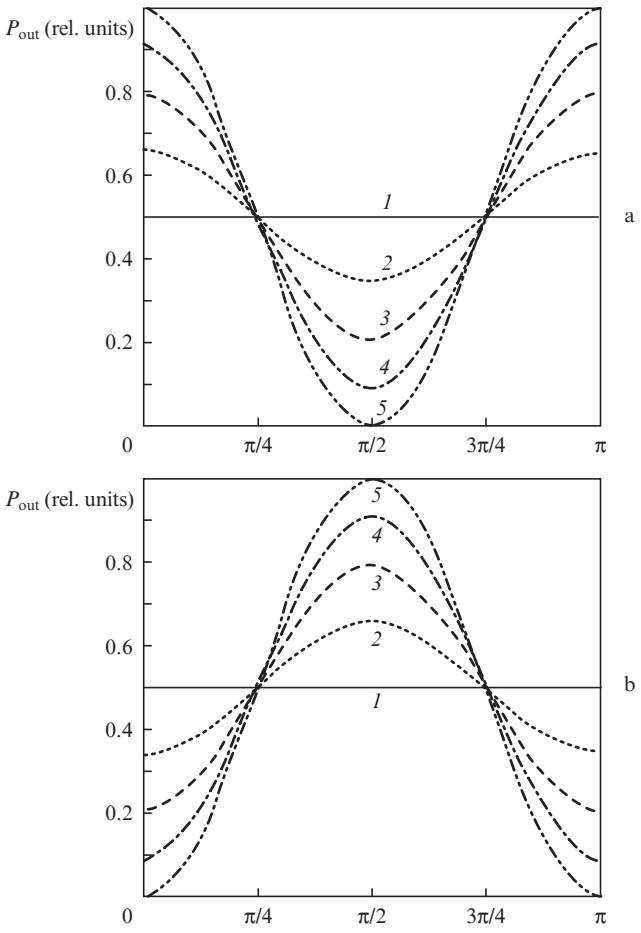

Figure 2. Dependences of the transmission P_{out} on the rotation angle of the output polariser a_3: (a) $h = 10.75\lambda/\Delta n$ (*1*), $10.8\lambda/\Delta n$ (*2*), $10.85\lambda/\Delta n$ (*3*), $10.9\lambda/\Delta n$ (*4*), $11.0\lambda/\Delta n$ (*5*) and (b) $h = 10.25\lambda/\Delta n$ (*1*), $10.3\lambda/\Delta n$ (*2*), $10.35\lambda/\Delta n$ (*3*), $10.4\lambda/\Delta n$ (*4*), $10.5\lambda/\Delta n$ (*5*).

$$P^{max}_{out} = P_{out}(a_3 = 0) = \frac{P_{in} t_1 t_2 t_3}{2}\left[1 + \cos\left(\frac{2\pi}{\lambda} h\Delta n\right)\right],$$
$$P^{min}_{out} = P_{out}(a_3 = \pi/2) = \frac{P_{in} t_1 t_2 t_3}{2}\left[1 - \cos\left(\frac{2\pi}{\lambda} h\Delta n\right)\right]. \quad (4)$$

Extracting the wave path length difference introduced by the crystal from Eqns (4), we obtain

$$h\Delta n = \frac{\lambda}{2\pi}\arccos\left(\frac{P^{min}_{out} - P^{max}_{out}}{P^{min}_{out} + P^{max}_{out}}\right). \quad (5)$$

Since the values of the arc cosine function lie within the limits $[0; \pi]$, the fractional part of the WPLD $h\Delta n \in [0; \lambda/2]$ can be calculated using Eqn (5).

Now let us calculate the WPLD measurement error for the minimum–maximum method. Assume that the maximal relative error of the measuring tract is $\pm\Delta P = \pm\Delta P_{in} \pm \Delta S$, including the relative power instability of the radiation source ΔP_{in} and the relative error of the photodetector ΔS. The calculations yield the expression for the relative error $\Delta(h\Delta n)$:

$$\Delta(h\Delta n) = \left| 1 - \arccos\left[\frac{(P^{min}_{out}/P^{max}_{out}) - 1 + \Delta P}{(P^{min}_{out}/P^{max}_{out}) + 1 + \Delta P}\right] \times \left(\arccos\left[\frac{(P^{min}_{out}/P^{max}_{out}) - 1}{(P^{min}_{out}/P^{max}_{out}) + 1}\right]\right)^{-1} \right|. \quad (6)$$

Note that $P_{out}^{min}/P_{out}^{max} \to 1$ at $h \sim \lambda/(4\Delta n)$ and $P_{out}^{min}/P_{out}^{max} \to 0$ at $h \sim \lambda/(2\Delta n)$.

In Eqn (6) the temperature variation of birefringence Δn is not taken into account, since the measurement time does not exceed a few seconds and the measuring system is placed in a thermostatically controlled case. The wavelength drift, λ, for stabilised radiation sources is also negligible (10^{-6}–10^{-8}).

Let us estimate the error of P_{out} due to imprecise adjustment of the angles a_1, a_2, a_3. The error of mutual alignment of the polariser and the crystal optical axis is characterised by the angle difference $a_{12} = a_1 - a_2$. The effect of a_{12} manifests itself in excitation of different power components $P_x \sim \cos^2(\pi/4 + a_{12})$, $P_z \sim \sin^2(\pi/4 + a_{12})$, polarised along the optical axes x and z. The composition of unequal components P_x and P_z at the output of the analyser increases the minimal value of the function $P_{out}(a_3)$ by $\delta P_{12} = P_z - P_x$. The corresponding relative error ΔP_{12} is expressed as

$$\Delta P_{12} = \frac{\delta P_{12}}{P_x + P_z} = \frac{\sin^2(\pi/4 + a_{12}) - \cos^2(\pi/4 + a_{12})}{\sin^2(\pi/4 + a_{12}) + \cos^2(\pi/4 + a_{12})} = \sin(2a_{12}).$$

For rotary mounts with vernier scale and micrometre screw the division value is 0.1°, which yields the error $\Delta P_{12} = 0.35\%$. This value can be reduced by 10–100 times using motor-driven mounts with the angle resolution 0.01°–0.001°.

The error of mutual alignment of the crystal and the analyser axes $a_{23} = a_2 - a_3$ shifts the plot of the function $P_{out}(a_3)$ along the a_3 axis, but does not affect the values P_{out}^{min} and P_{out}^{max} themselves. Hence, the error of the angle a_3 adjustment does not contribute to the error of WPLD measurement.

Now we estimate the error introduced by the discreteness of the rotary mount of the analyser δa_3. Its effect consists in imprecise tuning of the analyser at the minimum and maximum of the transmission $P_{out}(a_3)$. As a result the relative error $\Delta P_3 = 2\sin^2(\delta a_3/2)$ arises. For $\delta a_3 = 0.1°$ the error is $\Delta P_3 = 1.5 \times 10^{-4}\%$. Such a small error is explained by the fact that in the WPLD measurements we use gently sloping parts of the function $P_{out}(a_3)$.

Thus, the errors ΔP_{12} and ΔP_3 related to the adjustment of the angles a_1, a_2, a_3 appear to be significantly smaller than the instability of typical laboratory light sources and photodetectors that vary from 2.5% to 7%.

Figure 3 presents the dependences of the error (6) on the fractional part of WPLD at different model errors $\pm\Delta P$ of the measuring system.

Since the derivative of the function arccos(x) is maximal at $|x| \to 1$, the measurement error will be maximal at $P_{out}^{max} \gg P_{out}^{min}$, i.e., $h\Delta n \sim \lambda/2$. Substituting this condition into Eqn (6) and using the lower-order power series approximation, we obtain the maximal relative error in the form

$$\Delta(h\Delta n)_{max} \approx \frac{2\sqrt{\Delta P}}{\pi}. \quad (7)$$

In general-purpose power meters $\Delta S = \pm 0.11 \ldots \pm 0.25$ dB for the scale resolution 0.01–0.1 dB and the lower measurement limit from –60 to –70 dB. The instability ΔP_{in} in the stabilised semiconductor radiation sources is no worse than ±0.03 dB for 10 min. Then for the photodetector with the input aperture diameter 400 μm the signal power P_{out}^{max} is from –10 to –20 dB. Hence, it becomes possible to measure the fractional part of the WPLD with the error from $(\lambda/\Delta n)/10$–$(\lambda/\Delta n)/100$ and the resolution from $(\lambda/\Delta n)/30$ to $(\lambda/\Delta n)/300$.

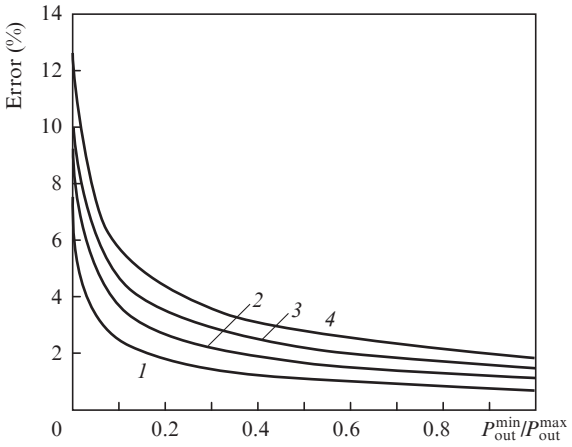

Figure 3. Relative error of WPLD measurement for ΔP= (*1*) 0.10, (*2*) 0.15, (*3*) 0.20 and (*4*) 0.25 dB.

For an adequate measurement of the ratio $P_{out}^{min}/P_{out}^{max}$ the optomechanical measuring scheme has to provide the necessary dynamic range. As practice shows, such setups provide the dynamic range of 30–40 dB, which allows future reduction of the WPLD measurement error from $(\lambda/\Delta n)/10$ to $(\lambda/\Delta n)/50$–$(\lambda/\Delta n)/150$ due to source stabilisation and precise calibration of the photodetector.

In the measurement it is necessary to account for the spectral transmission of the polariser–uniaxial crystal–analyser structure that has a periodic form [13]. The greater the crystal WPLD, the smaller the period of the spectral function. For example, for the lithium niobate crystal with the thickness h = 2 mm and the birefringence $\Delta n = 0.086$ at the wavelength λ = 633 nm, the period is 1.2 nm. Therefore, the measurement should be performed using a narrow-band frequency-stabilised radiation source.

Let us consider the measurement of the transmission phase function for a one-dimensional TDOE. We rewrite Eqn (3) taking the WPLD increment $\varphi(z)$ caused by the electric field into account. When measuring the phase function, the angle of rotation of the analyser with respect to the crystal optical axis is set equal to $a_3 = \pi/4$:

$$P_{out}(z) = \frac{P_{in} t_1 t_2 t_3}{2}\left\{1 + \cos\left[\frac{2\pi}{\lambda}(h\Delta n + \varphi(z))\right]\right\}. \quad (8)$$

To find $\varphi(z)$ from Eqn (8) we use two measurements, namely, $P_{out}(z)_{U=0}$ in the absence of the voltage and $P_{out}(z)_{U=V}$ with the voltage $U = V$:

$$\varphi(z) = \frac{\lambda}{2\pi}\arccos\left(\frac{P_{out}(z)_{U=V}}{P_{out}(z)_{U=0}} + \frac{P_{out}(z)_{U=V}}{P_{out}(z)_{U=0}}\cos\left(\frac{2\pi}{\lambda}h\Delta n\right) - 1\right) - h\Delta n. \quad (9)$$

The TDOE electrooptic material is chosen to be a uniaxial crystal of x-cut lithium niobate ($LiNbO_3$) of congruent composition. This crystal belongs to the trigonal symmetry class 3m and has nonzero electrooptic coefficients r_{13}, r_{22}, r_{31}, r_{51} [14]. In the studied x-cut crystal with the orientation of the z

axis perpendicular to the linear electrodes the nonzero electric field strength components are $E_x(x,z)$ and $E_z(x,z)$. Hence, the new refractive indices for the ordinary and extraordinary waves, propagating parallel to the x axis, are expressed as follows [14]:

$$n_o' = \frac{n_o}{\sqrt{1 + n_o^2 r_{13} E_z(x,z)}} \approx n_o - \frac{1}{2} n_o^3 r_{13} E_z(x,z),$$
$$n_e' = \frac{n_e}{\sqrt{1 + n_e^2 r_{33} E_z(x,z)}} \approx n_e - \frac{1}{2} n_e^3 r_{33} E_z(x,z). \quad (10)$$

With Eqn (10) taken into account, the variation in the WPLD function $\varphi(z)$ entering Eqn (8) for the x-cut lithium niobate takes the form:

$$\varphi(z) \approx \frac{1}{2}(n_o^3 r_{13} - n_e^3 r_{33}) \int_h E_z(x,z)\,\mathrm{d}x. \quad (11)$$

After the measurement of $\varphi(z)$ the electric field integral $\int_h E_z(x,z)\,\mathrm{d}x$ that enters Eqn (11) is calculated, making it possible to determine the TDOE phase functions $\varphi_o(z)$ and $\varphi_e(z)$ for the ordinary and extraordinary wave:

$$\varphi_o(z) \approx -\frac{\pi}{\lambda} n_o^3 r_{13} \int_h E_z(x,z)\,\mathrm{d}x = -\frac{2\pi}{\lambda} \frac{n_o^3 r_{13}}{n_o^3 r_{13} - n_e^3 r_{33}} \varphi(z),$$
$$\varphi_e(z) \approx -\frac{\pi}{\lambda} n_e^3 r_{33} \int_h E_z(x,z)\,\mathrm{d}x = -\frac{2\pi}{\lambda} \frac{n_e^3 r_{33}}{n_o^3 r_{13} - n_e^3 r_{33}} \varphi(z). \quad (12)$$

The approximation in Eqn (12) is determined by the substitution $1/(1 + r_{13} n_o^2 E_z)^{1/2} \approx 1 - 0.5 r_{13} n_o^2 E_z$ and $1/(1 + r_{33} n_e^2 E_z)^{1/2} \approx 1 - 0.5 r_{33} n_e^2 E_z$ performed in Eqn (10). For the lithium niobate ($n_o = 2.286$, $n_e = 2.200$ at $\lambda = 633$ nm and $r_{13} = 9.6$ pm V^{-1}, $r_{33} = 30.9$ pm V^{-1}) for the field strength E_z not exceeding the coercive field strength (2×10^7 V m^{-1}) the error introduced by this substitution does not exceed 4×10^{-4}%.

Thus, the proposed method allows the measurement of phase functions of one-dimensional TDOEs on the basis of uniaxial crystals with a linear electrooptic effect. This extends the possibilities of studying and constructing tunable focusing and deflecting optical elements.

The developed method is applicable in the absence of light diffraction at optical inhomogeneity regions in the volume of the electrooptic crystal, i.e., the tunable diffraction optical element should operate in the regime of Raman–Nath diffraction rather than Bragg diffraction. This fact imposes the following limitations on the spatial period of electrodes d and the radiation wavelength λ,

$$L \ll \frac{nd^2}{2\pi\lambda},$$

where L is the length of interaction between the radiation and the region of optical inhomogeneity induced by the field. To estimate L, we calculated the electric field distribution in the TDOEs on the basis of x-cut lithium niobate using the Comsol Multiphysics numerical simulation program. The results of the field calculation in the form of equipotential lines at d = 300 μm are presented in Fig. 4.

According to the calculation results, the field penetration depth is approximately equal to the period of electrodes, $L \approx d$. Thus for the lithium niobate-based TDOE the condition $d \gg 2\pi\lambda/n$ should be valid. For the wavelengths 0.5–1 μm this condition yields a lower boundary of tens of micrometres for the period of electrodes.

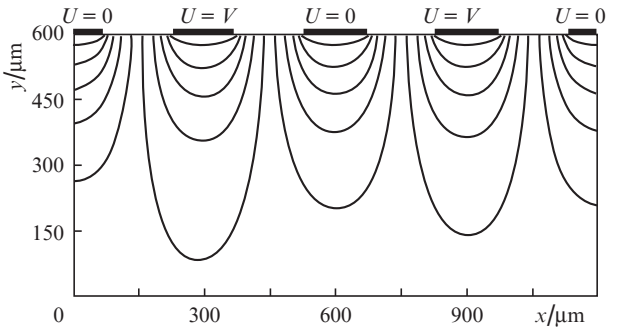

Figure 4. Distribution of the electric field potential U in the TDOE based on x-cut lithium niobate.

3. Experimental study

To test the WPLD measuring method we used the phase plates with $h\Delta n = \lambda/4$ and $h\Delta n = \lambda/2$, achromatised in the region 600–1100 nm with the manufacturing error no greater than $\lambda/(100\Delta n)$. The plate surfaces were bloomed to reduce the reflection to $R < 0.25$%. The plates were installed in rotary mounts with the division value of 2° and fixed after aligning by means of a micrometre screw.

The single-mode semiconductor laser diode with the radiation wavelength 639.4 nm and the divergence no greater than 0.1–0.2 mrad was used as a radiation source. The spectral bandwidth of the source did not exceed 0.02 nm. To prevent excitation of the laser diode by the reflected radiation we used a neutral filter with 10 dB attenuation, mounted after the source at the angle 45° to the optical axis. The radiation at the input and output of the phase plates was polarised by Glan–Taylor prisms.

The FOD-1202Si calibrated optical power meter operating in the range from +5 to –60 dB at the wavelength 650 nm served as a photodetector. The scale resolution was 0.1 dB, and the measurement error of the relative power levels did not exceed 0.25 dB.

For the etalon quarter-wave plate the dependence $P_{out}(a_3)$ was observed, which in correspondence with Fig. 2 is close to a horizontal line. According to Eqn (5), the measured value of the WPLD was $\lambda/(4\Delta n)$ (1.2%), which did not exceed the expected error ~2% (see Fig. 3).

For the half-wave plate a significant (up to 30 dB) modulation depth of the function $P_{out}(a_3)$ was observed. Using Eqn (5), the WPLD $\lambda/(2\Delta n)$ (15%) was obtained, which also keeps within the calculated error.

To study the phase function we used the electrooptic crystal of x-cut congruent lithium niobate having the dimensions 15×15×1 mm. The surface purity of the crystal corresponded to the class PIII according to the State Standard 11141-84, the surface nonflatness did not exceed 10″ and the roughness was smaller than 2 nm. The experimentally measured fractional part of the WPLD of the used electrooptic crystal amounted to $0.1(\lambda/\Delta n)$.

Linear electrodes were produced on a glass slide and had the period 300 μm and the interelectrode gap 175 μm. The electrode structure consisted of the adhesion layer of chromium with the thickness 10 nm and the upper layer of copper with the thickness 250 nm. The slide with electrodes on it was

glued to the crystal with the optical glue REO-113K, providing the electric isolation.

For the detailed study of the phase function we used a 10× objective with the numerical aperture 0.25. The images of the gaps were recorded with the CCD camera DCM 310 having the resolution 1024×768. The radiation source power deviation did not exceed ±0.05 dB. The high-voltage supply unit provided the control voltage 0–1000 V with pulsations no greater than 0.2 V. The voltage was measured using the GDM-78251 voltmeter with the error smaller than 0.012%.

Figure 5 presents the TDOE phase function measured using the proposed method under the voltage 1000 V. The potential distribution at the electrodes had the periodic form 00V00V.

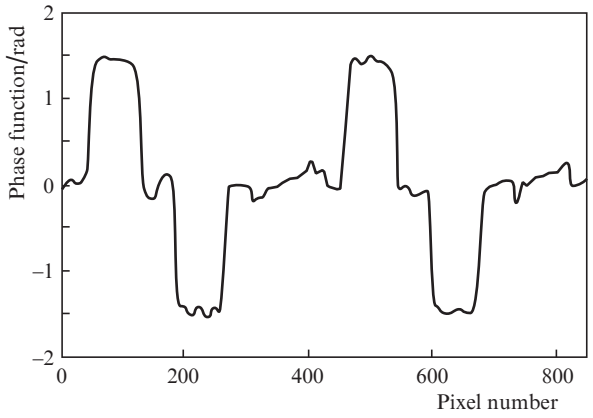

Figure 5. Phase function of the TDOE under the voltage 1000 V.

The phase function is seen to have a periodic form, the phase distribution over the gap being close to uniform. The sign of the phase variation was determined by the direction of the transverse electric field in the crystal, which is typical for the linear electrooptic effect of the first order. The nonzero phase function between the equipotential electrodes (pixel numbers 300–420 and 710–830 of the CCD matrix) is produced by the transverse electric field of the adjacent electrode pairs. The role of exactly the transverse field is confirmed by the opposite sign of the phase change at the edges of interelectrode gaps.

The application of voltage up to 1000 V to the interelectrode gap 175 μm wide did not produce optical inhomogeneities (domains), distinguishable with a polarisation microscope. The absence of needle-like domains, produced by the electric field along the optical axis of the lithium niobate crystal, is explained by the presence of an isolating glue layer between the electrodes and the crystal surface, confirmed by three-four interference fringes, observed after gluing the lithium niobate and the glass with the electrodes. The glue layer obstructs the injection of electrons into the surface layer of the crystal and the development of the domain structure.

To check the electric field distribution and the phase function, the numerical methods [15] were used with the following parameters of the lithium niobate crystal: $n_o = 2.286$, $n_e = 2.200$, $r_{13} = 9.6$ pm V^{-1}, $r_{33} = 30.9$ pm V^{-1}, $\varepsilon_x = 84$, $\varepsilon_z = 25$ [14, 16]. The calculated sensitivity of the phase function in the interelectrode gap was 1.51–1.52 mrad V^{-1}, which agrees well with the experimental values. Therefore, for the radiation power density 0.01–0.1 mW cm^{-2}, the wavelength 639.4 nm, the spectral bandwidth smaller than 0.02 nm and the electric field strength up to 5.7×10^6 V m^{-1} along the optical axis (the voltage 1000 V), the phase function of the TDOE on the basis of congruent lithium niobate is correctly described by the theory of the linear electrooptic effect and the numerical solution of the Laplace equation.

4. Conclusions

The method of phase function assessment in one-dimensional TDOEs is developed, based on measurements of the transmission of interelectrode gaps (polarisation of transmitted radiation). The proposed method allows the investigation of phase functions of one-dimensional TDOEs using the linear electrooptic effect in uniaxial crystals.

For the radiation power density 0.01–0.1 mW cm^{-2}, the wavelength 639.4 nm, the spectral bandwidth smaller than 0.02 nm and the electric field strength along the optical axis up to 5.7×10^6 V m^{-1}, the measured phase function of the TDOEs based on congruent lithium niobate agrees with the theory of the linear electrooptic effect and the Laplace equation. The absence of domain formation along the crystal optical axis is explained by the presence of the isolating glue layer that obstructs the injection of electrons into the surface layer of the crystal.

References

1. Ivanenko M. et al. *Proc. SPIE Int. Soc. Opt. Eng.*, **7194**, 7194-06 (2009).
2. Qing Y. et al. *Opt. Express*, **15** (25), 16933 (2007).
3. Qing Y. et al. *Opt. Lett.*, **36** (13), 2453 (2011).
4. Robinson M.G. et al. *United States Patent 'Diffractive Spatial Light Modulator'* No. 6091463; date of patent Jul. 18, 2000.
5. Stappaerts E.A. et al. *United States Patent 'Longitudinal PLZT Light Modulator'* No. 5221989; date of patent Jun. 22, 1993.
6. Sun D., Zhao C., Chen R. *Appl. Opt.*, **3** (3), 629 (1997).
7. Knop K., Kane J. *United States Patent 'Tunable Diffraction Subtractive Filter'* No. 4251137; date of patent Feb. 17, 1981.
8. Kulishov M. *J. Lightwave Technol.*, **21** (3), 854 (2003).
9. Tatebayashi T., Yamamoto T., Sato H. *Appl. Opt.*, **31** (15), 2770 (1992).
10. Valley P. et al. *Proc. SPIE Int. Soc. Opt. Eng.*, **7786**, 77860H-01 (2010).
11. Shubnikov A.V. *Osnovy opticheskoy kristallografii* (Fundamentals of Optical Crystallography) (Moscow: Izd. Akad. Nauk SSSR, 1958).
12. Chetverikov S.D. *Metodika kristallograficheskogo issledovaniya shlifov* (Methods of Crystallographic Study of Thin Sections) (Moscow: Gosgeolizdat, 1949).
13. Paranin V.D., Matyunin S.A. *Datchiki i Sistemy*, **7**, 59 (2013).
14. Yariv A., Yeh P. *Optical Waves in Crystals* (New York: Wiley, 1984).
15. Samarskii A.A., Gulin A.V. *Chislennye metody: uchebnoye posobiye dlya vuzov* (Numerical Methods: A Tutorial for Institutes of Higher Education) (Moscow: Nauka, 1989).
16. Burkhanov A.I. et al. *Tez. Mezhdunarodnoy nauchno-tekhnicheskoy konferentsii INTERMATIC-2011* (Proc. Int. Sci. Tech. Conf. INTERMATIC-2011) (Moscow, 2011) Vol. 2, pp 110–113.